Charge exchange in low-energy proton-surface scattering studied by discrete variational $X\alpha$ cluster calculations

R. Souda, K. Yamamoto, B. Tilley,* W. Hayami, T. Aizawa, and Y. Ishizawa

National Institute for Research in Inorganic Materials, 1-1 Namiki, Tsukuba, Ibaraki 305, Japan

Neutralization and electronic excitation during low-energy proton-surface scattering have been investigated from a combination of experiments and discrete variational $X\alpha$ calculations of the adiabatic molecular-orbital-energy diagram. The charge exchange in D^+ scattering seems to have a more local character than expected from the conventional band picture of resonance neutralization, especially for the ionic-compound surfaces or surfaces with positively or negatively charged adatoms. Some of these local features are shown to arise from the formation of the surface molecule or the promotion of the H $1s$ orbital during the violent collision, which results in electronic excitation, such as reionization or electron-hole pair formation, and suppression of ion neutralization to some extent. The experimentally observed target-element dependencies of these processes are elucidated qualitatively in line with this scheme.

I. INTRODUCTION

In the past two decades, low-energy ion scattering (LEIS) has been developed as a powerful technique for compositional and structural analysis of solid surfaces. The extreme surface sensitivity of LEIS is caused mainly by the efficient ion neutralization effects at a surface and, therefore, a better understanding of the charge-exchange process is an inevitable prerequisite for a quantitative discussion of the experimental results. It is well established that an ion captures a surface electron via resonant-tunneling (RT) and Auger-neutralization (AN) processes.[1-4] The relative role of these processes is sensitively dependent on the energy position of the ion vacant level relative to that of the target valence band. Moreover, the projectiles once neutralized can be reionized either via RT or via the electron-promotion mechanism during the violent collision.[5,6] Thus, the charge exchange should be a quite complicated process to which several mechanisms can contribute in various situations. So far, a considerable research effort has been devoted to alkali-metal ions and noble-gas ions, but few investigations had been made of the other ions which might be classified as "reactive" ions. Among them, hydrogen is of particular interest since it is the simplest projectile and its neutralization behavior is known to be unique.[7] In general, ions scattered from the outermost surface layer are more likely to survive neutralization than those scattered from the bulk, and form surface peaks in their energy distributions. This is, in fact, the case for rare-gas ions such as He^+. However, the surface peak of H^+ or D^+, though clearly recognized for surfaces of perfectly ionic compounds like alkali halides, is almost completely absent for metal and semiconductor surfaces.[8] In view of such a remarkable chemical effect on neutralization of D^+, an experimental approach to investigate the bond nature of solid surfaces has been developed recently.[9,10]

The aim of this paper is to discuss the mechanism of charge exchange and electronic excitation in proton-surface interactions. It is recognized that the response of the surface electronic system to a moving ion is highly dynamic and, hence, the charge-transfer probability is often calculated by using the time-dependent Newns-Anderson model.[3] In this framework, the effect of the valence-band width on the charge-exchange probability (band effect) has been suggested.[11-14] From the experimental point of view, however, there are some indications that charge transfer in D^+ (H^+) scattering has a more local character depending on the species of target atoms.[8-10] In order to gain better insight into the charge-exchange phenomena, we have calculated electronic structures for D^+ (H^+) interacting with various surface clusters by using self-consistent-charge discrete variational $X\alpha$ (SCC-DV-$X\alpha$) methods. It will be shown that such adiabatic energy-level calculations for stationary states are also very successful for qualitative understanding of the dynamical charge-transfer process.

II. EXPERIMENT

The experiments were made in an ultrahigh vacuum (UHV) chamber equipped with facilities for LEIS, ultraviolet photoelectron spectroscopy, low-energy electron diffraction (LEED), and a load-lock system for sample transfer. The D^+ ion was generated in a discharge-type ion source and was mass analyzed by using a Wien filter. Ions with kinetic energy E_0 ranging from 10 eV to 1 keV could be incident upon a surface with an angle of 80° from the surface. Ions scattered specularly through a laboratory scattering angle of 160° were detected by means of a hemispherical electrostatic energy analyzer operating with a constant energy resolution of 1 eV.

So far, D^+-scattering experiments have been performed for a variety of solid surfaces[8-10] such as metals [Ag, Pt(111), Ta(111), W(110), etc.], elemental semiconductors [Si(001), Ge(001), diamond(001), etc.], and ionic compounds [NaCl, NaI, KF, KI, CsF, CsCl, MgO(001), BaO, BaF$_2$(111), etc.]. Among them, the results of

MgO(001), NaCl, and CsF are displayed explicitly here. A sample of MgO with a (001) face was introduced into the UHV chamber immediately after cleavage in air, and was then heated by electron-beam bombardment up to 800 °C. The surface thus prepared showed an excellent 1×1 pattern in LEED. The other samples were polycrystalline thin films evaporated *in situ* on substrates of hydrogen-terminated Si(001) surfaces. The charging effect during ion-beam bombardment of the MgO(001) surface was successfully suppressed by decreasing the ion-beam current and by heating a Ta filament placed just behind the sample.

III. RESULTS AND DISCUSSION

A. Metal and elemental-semiconductor surfaces

In the literature,[8-10] it has been shown that surface peaks are almost completely absent in H^+ or D^+ scattering from metal surfaces, although they are prominent in the energy spectra of He^+ scattering. The same is essentially true for semiconductor surfaces such as Si(001) and Ge(001). It is believed that He^+ ions are neutralized mainly via the AN process because of the large energy separation between the He 1s level and the valence band. On the other hand, the 1s level of D^+ (H^+) is located so close to the valence band that the RT process may also contribute to neutralization. Indeed, we have attributed the large difference in the neutralization probability of D^+ and He^+ scattering to the dominant contribution of RT in the former.[8-10] In order to confirm this assumption, the molecular orbital (MO) calculations are performed for H^+ (D^+) interacting with these surfaces.

The MO energy-level diagram is numerically calculated with the use of the SCC-DV-$X\alpha$ method; the strategy of the calculation has been shown elsewhere.[15,16] Briefly, the Hartree-Fock-Slater (HFS) equation for a cluster is solved self-consistently with the use of a localized exchange potential ($X\alpha$ potential). The exchange correlation parameter α is adjustable and is taken as 0.7. Numerical atomic orbitals, obtained as solutions of the atomic HFS equations, were used as basis sets.

Figure 1 shows the energy-level diagram for the $(Al_{10}H)^+$ cluster, which simulates H^+ approaching Al(111) from the surface normal. The electronic structure of the surface calculated by using the Al_{10} cluster is also shown on the right-hand side of the figure. The cluster model used in the calculation is schematically indicated in the inset. The energy levels are plotted in Fig. 1 so that the energy-level variations of the valence orbitals with the H 1s component can be surveyed as a function of the separation d of hydrogen from the target Al atom; the population of the H 1s atomic orbital in each valence orbital is indicated by the length of the horizontal bar. The distribution of the H 1s component over the wide energy range of the band indicates the existence of a strong orbital hybridization between H 1s and the Al sp band, although the H 1s orbital is highly promoted if the separation is below 1.5 a.u. The survey of the energy-level variations shown here is useful for determination of the static chemisorption state of hydrogen. The 1s orbital ac-
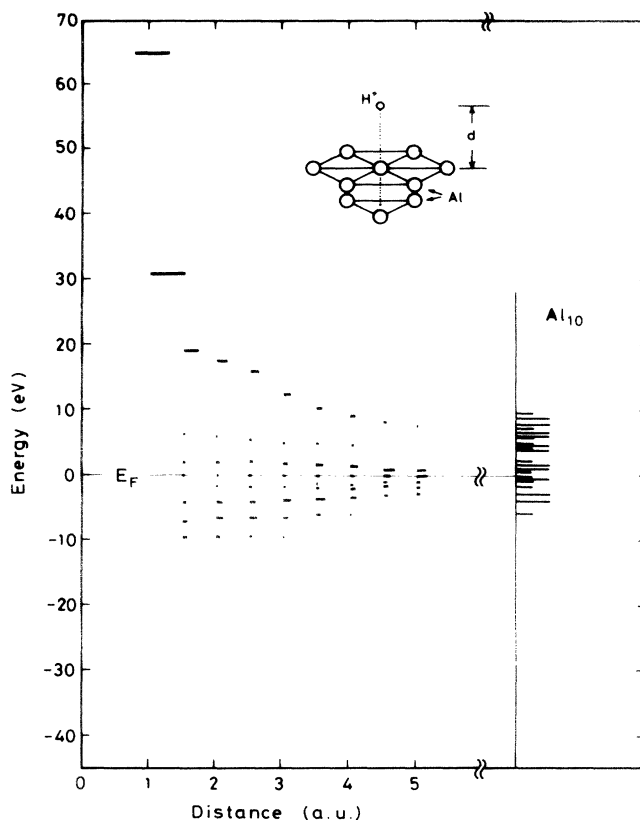

FIG. 1. The energy-level diagram for the $(Al_{10}H)^+$ cluster simulating H^+ scattering from the Al(111) surface. The valence orbitals with a H 1s component is shown as a function of the internuclear distance between H^+ and the center Al atom in the cluster. The bar length indicates the H 1s orbital population in each molecular orbital. The energy levels for the Al_{10} cluster are also shown.

commodates two electrons and the states located below E_F are occupied. The net charge of hydrogen is thus determined as -0.07 to -0.18 for $2 < d < 5$ a.u., suggesting the occurrence of a slightly negatively charged state at the on-top site, if possible, of the Al(111) surface.

The calculation is also done for the $(Si_4H_{10})^+$ cluster to simulate H^+ scattering from a Si surface with a dangling-bond state. The calculated results are shown in Fig. 2. The bonds of all silicon atoms at the edge of the cluster were saturated with hydrogen atoms so as not to leave any other dangling-bond states. The results are quite similar to those for the $(Al_{10}H)^+$ cluster.

The distance of the closest approach, R_c, for D^+ colliding with various target species discussed here is shown in Fig. 3 as a function of the kinetic energy E_0. The calculation is made by using the Moliere approximation to the Thomas-Fermi potential with scattering radius reduced by 20%. The R_c value for $E_0 = 100$ eV D^+ ranges from 0.6 a.u. (O) to 1.1 a.u. (Cs).

The above discussion leads to the conclusion that a proton (deuteron) impinging upon a surface does capture a valence electron via RT and is neutralized with a high probability if the equilibration occurs. In reality, howev-
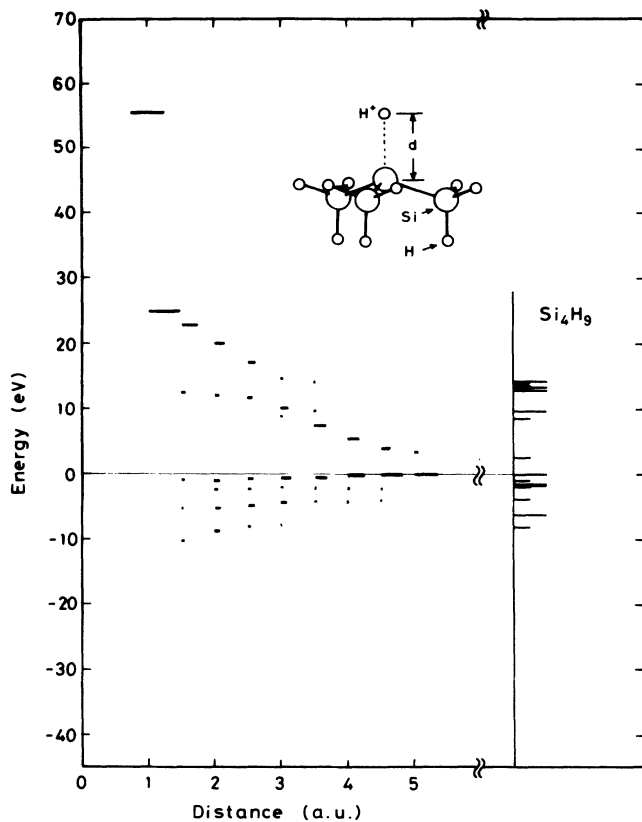
FIG. 2. Same as in Fig. 1 for the $(Si_4H_{10})^+$ cluster.
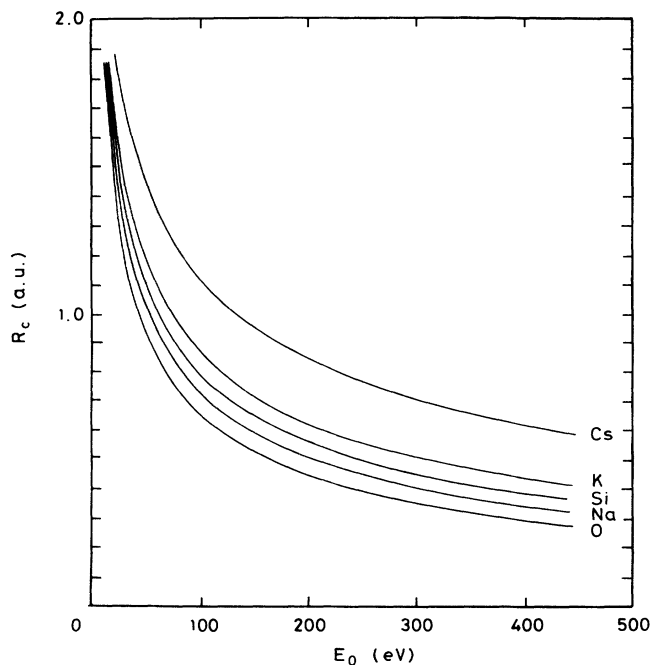

FIG. 3. The minimum impact distance R_c for D^+ colliding with O, Na, Si, K, and Cs atoms calculated by using the Thomas-Fermi-Moliere potential as a function of the kinetic energy E_0.

er, the ion neutralization is highly dynamical and its probability is determined by two competitive factors. One is, of course, the duration of the ion-surface interactions, $T \sim 10^{-15}$ sec, and the other is the transition rate ω of the valence electron. The broadening of the H $1s$ orbital distribution (Δ), caused by orbital hybridization with the valence band, is related to ω via the uncertainty principle, $\Delta = \hbar\omega$. According to the dynamical calculations,[3,11-14,17] the final charge state of H^+ can be obtained from the time evolution of the H $1s$ wave function by integrating ω along the whole scattering trajectories. It should also be noted that hydrogen favors a positively charged state in a close encounter due to a larger bonding/antibonding splitting. This state is the so-called "surface molecule" which is defined in the literature by Tsuneyuki, Shima, and Tsukada[13] as a possible localization mechanism of the hole. We will not perform the dynamical calculations here, but the neutralization probability can be scaled by the lifetime τ ($=1/\omega$) of the electron (hole) which is given approximately by

$$\tau = \hbar/W ,$$

where W indicates the valence-band width. Indeed, not only the transition rate ω of the H $1s$ hole to the band, but also the lifetime of the hole diffusing into the band, should be correlated to W. The experimental fact that D^+ is almost completely neutralized at metal and semiconductor surfaces shows that charge equilibrium is established in the course of scattering. This is due to the high mobility of the valence electron.

B. Ionic-compound surfaces

Neutralization should be suppressed for D^+ scattered from ionic compounds since the band width is fairly narrow compared to that of the metals or the semiconductors. In fact, one can confirm this from the body of experimental results published so far.[8] The bond ionicity of surface atoms is shown to be correlated to the appearance of surface peaks of D^+ surviving neutralization; large ionicity in the bonding of the alkali halides is manifested by the existence of intense surface peaks, whereas the surface peaks, even of oxides or halides, of the cationic species on the right-hand side of the Periodic Table (e.g., MgF_2, Al_2O_3, SiO_2, TiO_2, $MnCl_2$) are not remarkable. These results may be understandable within the framework of the band effect on the RT process. However, unresolved questions remain in some cases concerning the surface-peak intensity of cations relative to anions, and the energy-loss fine stuctures of the surface peak. In the case of dilute chemisorption systems such as oxygen and alkali metals on metal and semiconductor surfaces, neutralization of D^+ exhibits a considerable local character, which depends on the local bond nature between the adatom and the coordinating surface atoms, rather than the band structure of the substrate.[9,10] In what follows, some of the experimental results are presented to envisage the possibility of local charge exchange.

Figure 4 shows the energy spectrum of $E_0 = 200$ eV D^+ ions scattered from NaCl. The arrows on the abscissa indicate the position of the elastic binary-collision en-
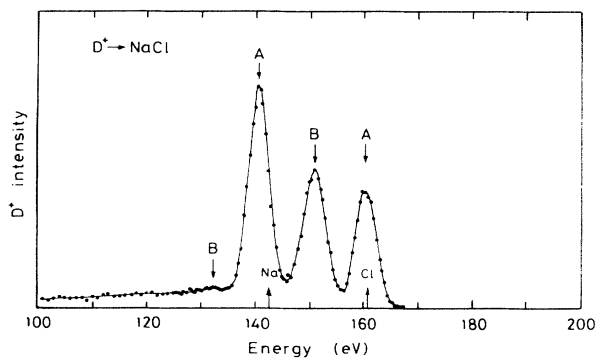
R. SOUDA *et al.*

FIG. 4. The energy spectrum of $E_0 = 200$ eV D$^+$ ions scattered from the polycrystalline NaCl surface. The energies corresponding to elastic binary collision with individual target atoms are indicated by arrows on the abscissa.

ergy for each target atom. The surface peaks for the constituent Na and Cl atoms are clearly recognized. The surface peak of Cl is composed not only of the elastic peak A but also of the energy-loss peak labeled B, whereas, for Na, peak B is quite small in intensity relative to peak A. There are at least two possible processes which could result in such inelastic energy loss during ion scattering: one is electron-hole-pair excitation and the other is reionization $(D^+ \rightarrow D^0 \rightarrow D^+)$. Peak B is assignable to *e-h* pair excitation because of the good correlation between the energy-loss value and the band-gap energy.[8] Shown in Fig. 5 is the energy spectrum of $E_0 = 100$ eV D$^+$ scattered from CsF. It is notable that the surface peaks are superposed on an extended background shown by the broken line, and the intensity of peak B is quite large relative to peak A. One of the questions to be solved here is why the energy-loss structure of the surface peak is so specific to the target atom.

Figure 6 shows the energy spectrum of D$^+$ ($E_0 = 200$ eV) scattered from the MgO(001) surface. In contrast to the results for the alkali halides, the Mg peak is almost completely absent. It is remarkable that the O peak is clearly seen despite the complete absence of the Mg peak. The apparent incompatibility of this peak distribution with the bond picture of RT, where the surface is as-
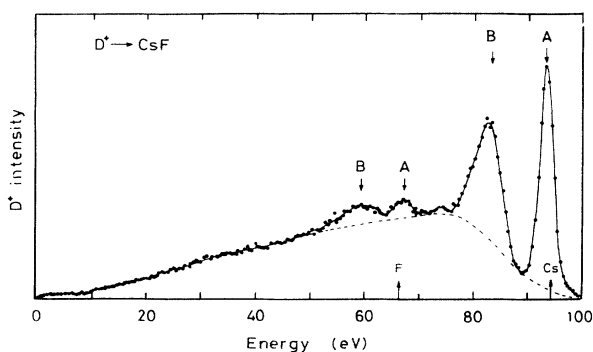

FIG. 5. The energy spectrum of $E_0 = 100$ eV D$^+$ ions scattered from the polycrystalline CsF surface.
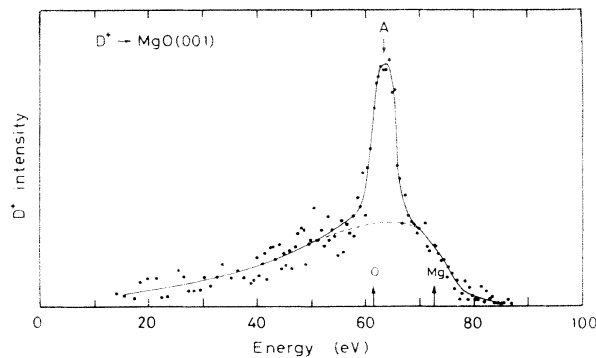

FIG. 6. The energy spectrum of $E_0 = 100$ eV D$^+$ ions scattered from the MgO(001) surface.

sumed to be a continuum of an electron sea, is another question.

1. Resonance neutralization

In this subsection, we contrive to explain the target-element dependence of neutralization by using MO energy diagrams. The calculations were made by using $(MX_5 H)^{(4n-1)-}$ and $(XM_5 H)^{(4n+1)+}$ clusters to simulate H$^+$ scattering from cations (M^{n+}) and anions (X^{n-}) of NaCl-type ionic-compound surfaces, where the electrostatic potentials from ions outside the cluster are also introduced according to the procedure described in the literature.[16] The results for H$^+$ on $(NaCl_5)^{4-}$, $(MgO_5)^{8-}$, $(KF_5)^{4-}$, and $(CsF_5)^{4-}$ are displayed in Figs. 7–10; the energy position of the valence orbital with the H 1s character, and the energy-level structure of the substrate, are indicated relative to the valence-band-top [or the highest occupied molecular orbital (HOMO)] positions. In all cases, the H 1s orbital component is distributed in the energy range corresponding to the valence band, indicating the formation of the bound state. The exception is the close encounter, where the major portion of H 1s appears apart from the valence band. The H 1s orbital promotion is caused by antibonding interaction with the target core (ns, np) orbitals as evidenced by the downward shift of the correlated bonding orbitals. It should be noted that the degree of the promotion is specific to the target elements, and the critical projectile-target separation for the onset of the promotion is increased if the target core orbitals become shallower in energy position and/or larger in spatial expanse. The occurrence of the H 1s orbital promotion is identical to the formation of the surface molecule described in the preceding section.

Although the hybridization of the H 1s orbital with the target core orbital may be partially responsible for neutralization, such a core orbital should only have a marginal effect on the neutralization probability because of the localized nature of the electron. Therefore, attention should be focused on the shallowest valence-band states. The results of MgO and NaCl are notable since the effect of the valence-band width on the neutralization probability can be singled out from other factors such as the formation of the surface molecule, as is seen in Figs. 7 and 8. Indeed the absence (presence) of the Mg (Na) surface peak shown in Fig. 4 (Fig. 6) can be ascribed to the band effect. The H 1s orbital distribution $(\Delta \sim W)$ is broader
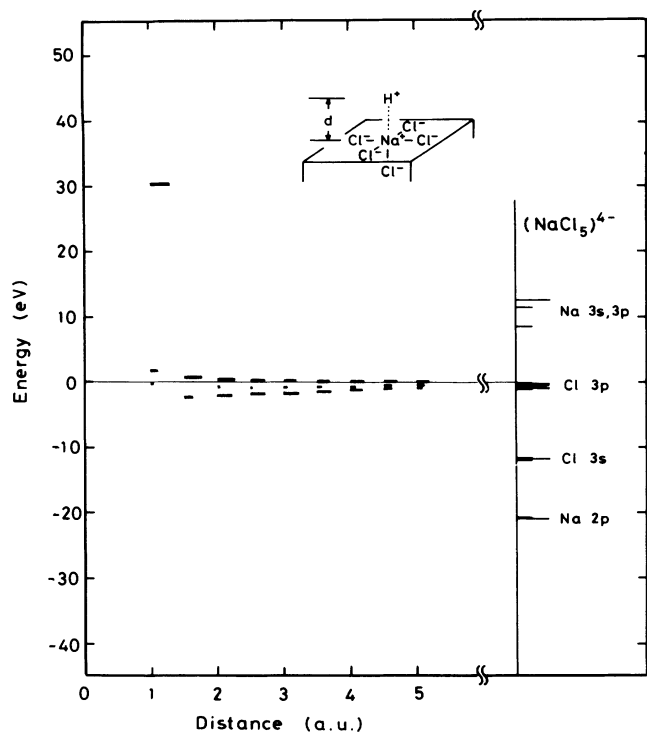
FIG. 7. Energy-level diagram for the $(NaCl_5H)^{3-}$ cluster simulating H^+ scattering from Na^+ of the NaCl(001) surface. The H $1s$ orbital component is shown as a function of the internuclear distance. The energy-level structure for the $(NaCl_5)^{4-}$ cluster is shown on the right-hand side.
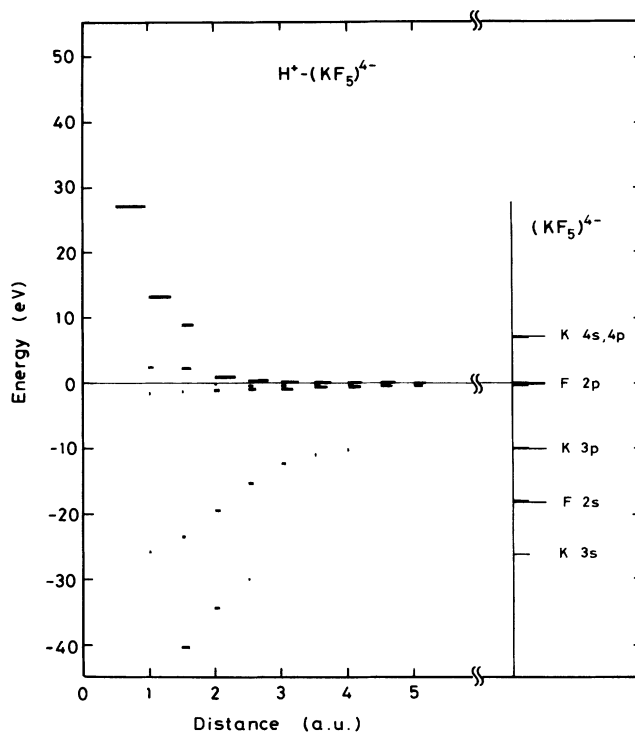
FIG. 9. Same as in Fig. 7 for the $(KF_5H)^{3-}$ cluster.

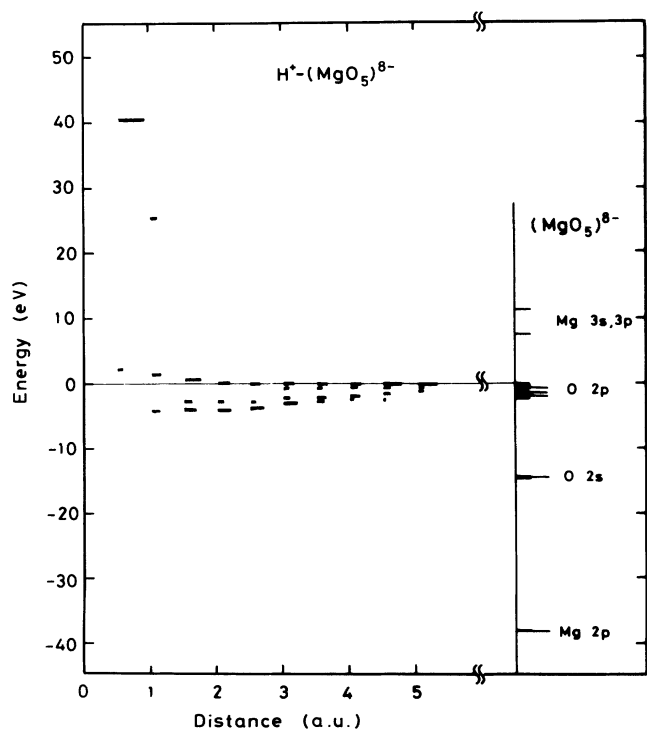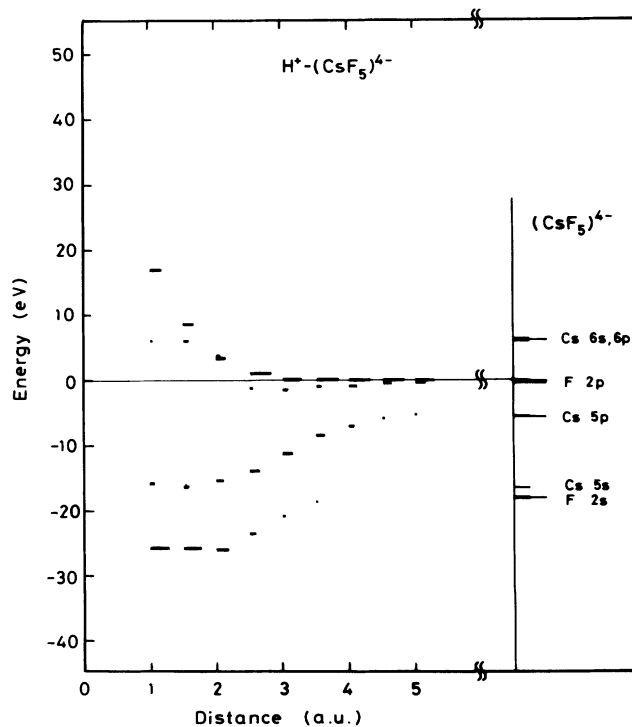FIG. 8. Same as in Fig. 7 for the $(MgO_5H)^{7-}$ cluster simulating H^+ scattering from Mg^{2+} of the MgO(001) surface.

FIG. 10. Same as in Fig. 7 for the $(CsF_5H)^{3-}$ cluster.

for MgO than for NaCl, suggesting smaller lifetime of the hole in MgO. In the case of D^+ scattering from the KF and CsF surfaces, much stronger localization of the $1s$ hole is inferred from much narrower W. Experimentally, intense surface peaks of K and Cs are observed.

The capture of a valence electron in D^+-anion collision is intuitively thought to occur more easily than that in D^+- cation collision, because the valence electron is spatially localized at the anion site. However, this simple picture should be discarded after considering the experimental results for MgO(001), where the O peak is clearly recognized despite the complete absence of the Mg peak. In terms of the energy-level calculations for H^+ on $(ClNa_5)^{4+}$ and $(OMg_5)^{8+}$ shown in Figs. 11 and 12, the H $1s$ orbital has an antibonding character and is promoted even at a fairly large separation compared to the H^+- cation collisions. The net charge of hydrogen is estimated as $+0.61$ (Cl^-) and $+0.95$ (O^{2-}) at $d = 5$ a.u. The bottleneck of the hole diffusion via oxygen into the band of MgO is thus caused by the formation of the surface molecule, D^+-O^{2-}. Of particular interest in this respect is the chemisorbed oxygen on the transition-metal surfaces such as Mo(111) and Ta(111), where the surface peak for O is prominent in the D^+ energy spectra irrespective of the wide metallic band of the substrate.[8]

2. Inelastic scattering

With regard to electronic excitation, the energy-level promotion mechanism has been utilized for many atomic
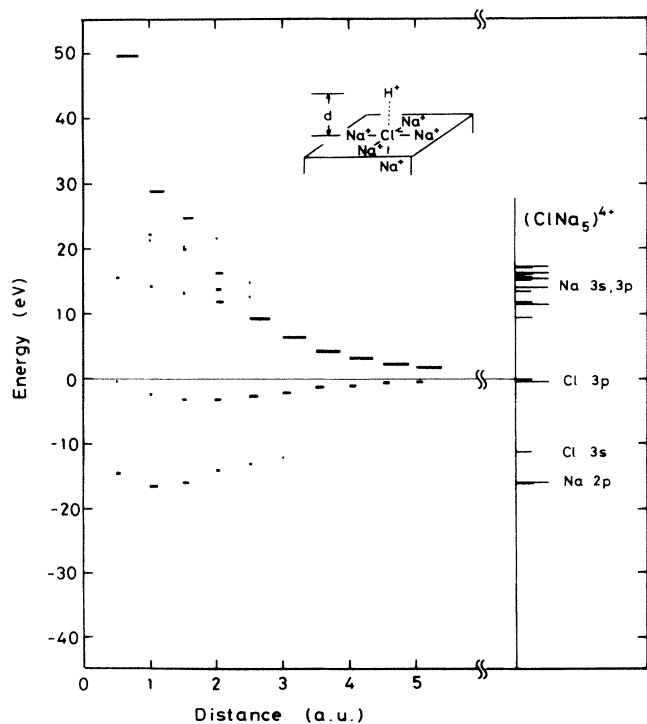

FIG. 11. The energy-level diagram for the $(ClNa_5H)^{5+}$ cluster simulating H^+ scattering from Cl^- at the NaCl(001) surface. The H $1s$ component is shown as a function of the internuclear distance between H^+ and Cl^-. The energy levels calculated for the $(ClNa_5)^{4+}$ cluster are also shown.
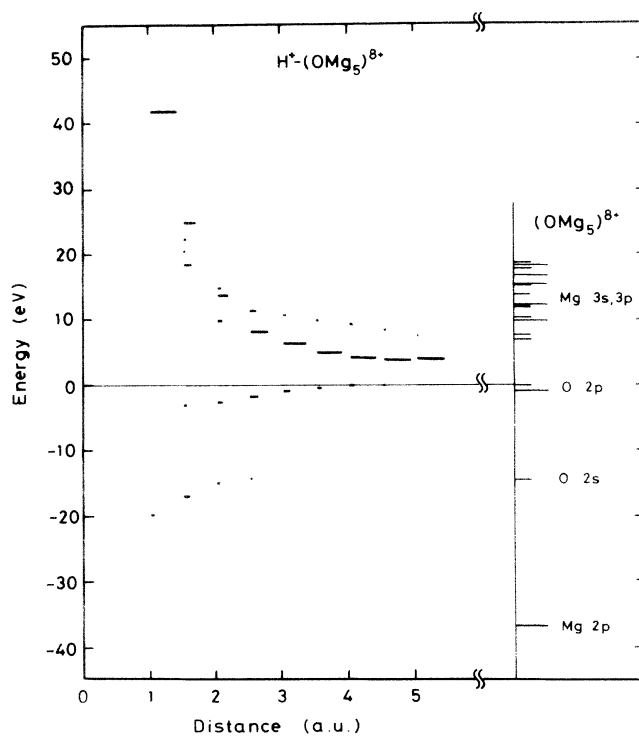

FIG. 12. Same as in Fig. 11 for the $(OMg_5H)^{9+}$ cluster.

collision processes.[18,19] The concept of the diabatic correlation diagram (DCD) has been introduced by Barat and Lichten[19] for heteronuclear diatomic collisions, where the electron transition occurs at the crossing point of the diabatic molecular orbitals which is drawn in separated-united atom diagrams by conserving the number of radial nodes, $n - l$. So far, DCD has been successfully applied to core-electron excitation in ion scattering.[20-22] However, it is likely that DCD is not applicable for valence-electron excitation. Moreover, it has recently been shown[23,24] that DCD fails to explain the reionization probability of He ($He^+ \rightarrow H^0 \rightarrow He^+$), especially for highly heteronuclear-collision systems: Tsukada, Tsuneyuki, and Shima[23] and Tsuneyuki and Tsukada[24] have made the unrestricted Hartree-Fock self-consistent field calculation, and the configuration interaction calculation, of a large number of molecular orbitals to discuss the target-material dependence of the reionization of He^0. As the MO calculation gives only a stationary state in which energy-level crossing is avoided, they determined the diabatic level crossing by inspection.

The energy-level diagrams calculated here exhibit a marked promotion of the H $1s$ orbital, which can be related to electronic excitation during ion scattering. In what follows, we intend to explain the e-h pair excitation by using calculated MO energy diagrams combined with the RT mechanism. Schematically shown in Fig. 13 is the proposed mechanism of e-h pair excitation. The H $1s$ orbital shifts upwards due to the image-charge effect and then a short-lived ($\sim 10^{-15}$ sec) chemisorption state is formed. On the incoming trajectory, if the valence electron is transferred to the H $1s$ orbital [resonance neutral-
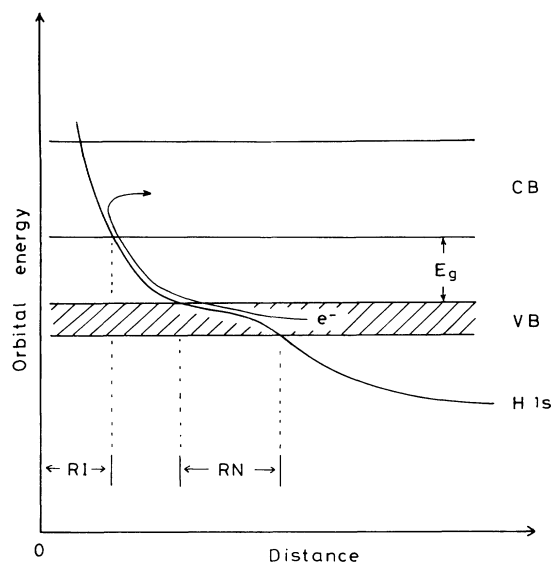
FIG. 13. A schematic view of the electron promotion mechanism in H^+-surface scattering. The H $1s$ orbital hybridizes the valence band (VB) at a certain internuclear distance. The valence electron can be promoted along the antibonding molecular orbital with a H $1s$ character provided that the charge equilibrium is (in part) achieved due to resonance neutralization (RN). Since the promotion is followed by the resonance ionization (RI) or the irreversible diffusion of the electron into the empty conduction band (CB) states, the electron-hole pair is finally created. Reionization, on the other hand, is such that the electron capture occurs a little far from the target-atom position where the H $1s$ orbital promotion takes place.

ization (RN)], the electron can be promoted along the antibonding molecular orbital. This is followed by ionization [resonance ionization (RI)] due to electron diffusion into the conduction band states. If the resultant ions survive RN on the outgoing trajectory, they finally form peak B in the energy spectra. These ions lose kinetic energy corresponding approximately to the band gap. The energy level diagrams for the H^+-K^+ (Fig. 9) and H^+-Cs^+ (Fig. 10) collisions show marked but gradual promotion of the antibonding MO, offering enough time for electron diffusion into the conduction band. By contrast, the promotion is rather sudden and occurs only at a closer encounter for the H^+-Na^+ collision (Fig. 7) so that the electron transition rate should be suppressed. The validity of this model is confirmed from the experimental results that intensity of peak B relative to peak A, though small for Na (NaCl, NaI), is fairly large for K (KF, KI) and Cs (CsF, CsCl). A similar tendency is found for chemisorption of Cs, K, and Na on the Si(001) surface as well.[9]

In the case of the H^+-Cl^- (Fig. 11) and H^+-O^{2-} (Fig. 12) collisions, a large gap opens between the antibonding MO [the lowest unoccupied MO (LUMO)] and the HOMO at moderate separations, so that the occupation of the LUMO can be suppressed to some extent. This effect may be responsible for the dominance of peak A for oxygen of MgO(001). In contrast, the O peak for oxy-

genated Mo(111) and Ta(111) surfaces seems to be composed mostly of the energy-loss peak (the peak position is about 6 eV lower than that of peak A of MgO),[8] which indicates that the occupation of the LUMO occurs with a relatively large probability compared to the highly ionic MgO surface. As for the oxygenated Pt(111) surface, no appreciable O peak is recognized[9,10] probably because the O-Pt bond has less ionicity. Indeed, the MO calculations for H^+ on the O-chemisorbed Pt(111) surface show no marked HOMO-LUMO gap for $d > 3.0$ a.u. and the probability for RN is thought to be enhanced due to the band effect of the Pt surface.[25]

It is shown in the literature[8] that the intensity of peak B relative to peak A for Cl at LiCl is dependent upon the primary energy of D^+ and decreases dramatically if E_0 is decreased below 20 eV.[8] The MO energy diagram for D^+ colliding with a $(ClLi_5)^{4+}$ cluster is quite similar to that shown in Fig. 5. The minimum impact distance of 20-eV D^+ on Cl is estimated to be about 2 a.u., which is in good agreement with the crossing point of the LUMO with the conduction-band states. It is thus concluded that the onset of the MO energy level crossing causes a certain threshold energy for the e-h pair excitation which is specific to the target atom.

The mechanism of the e-h pair excitation shown in Fig. 13 is basically identical to that of reionization $(D^+ \rightarrow D^0 \rightarrow D^+)$. We define reionization such that deuterium, being neutralized at a position far from the target atom via the RN or AN process, is ionized during collision, whereas, for e-h pair excitation, RT (RN and RI) takes place at the same atom (or cluster). Because the incidence of D^0 rather than D^+ is more realistic, reionization may be simulated by using a cluster with an excess electron. The calculated MO energy diagram for reionization also shows $1s$ orbital promotion similar to that explicitly shown here. The backgrounds of the D^+ energy spectra, seen in Figs. 4-6, are typical of reionized D^0. They are ejected from the surface after being neutralized in the deeper layers and then ionized during collision with the topmost-layer atoms just before leaving the surface.

Last, the effect of the cluster size on the calculated results, especially for H^+-Cl^- and H^+-O^{2-} collisions, should be addressed briefly. The results obtained using simpler $(ClH)^0$ and $(OH)^-$ clusters are almost the same as those shown in Figs. 11 and 12, respectively, except that the net charge of hydrogen (positive) is slightly decreased. By contrast, if the calculation is made for larger clusters $[(Cl_9Na_9H)^+$ and $(O_9Mg_9H)^+]$ which involve the second nearest-neighbor anions, the HOMO-LUMO gap narrows considerably at the larger separation $(d > 3$ a.u.). If that is the case, the electron can easily be transferred to LUMO, so that the intensity of peak B relative to peak A should be increased dramatically. In this case, the Mulliken population analysis reveals that a considerable amount of charge (2–3 electrons for NaCl and 4–5 electrons for MgO) flows to the fundamental $(XM_6H)^{n+}$ cluster from the outside. By considering the fact that the charge exchange interaction lasts only for a very short period ($\sim 10^{-15}$ sec), such a remarkable charge redistribution is unlikely to occur especially at the highly ionic

compound surfaces described here. However, such charge redistribution might be possible at a metal surface with relatively large electron mobility. The effect of the cluster charge on neutralization of D^+ will be discussed in detail elsewhere.[26]

IV. CONCLUSION

The electronic transition in low-energy D^+ scattering from surfaces with different electronic structures has been discussed on the basis of the molecular-orbital-energy diagrams calculated by using the DV-$X\alpha$ method, with a special emphasis placed on the local charge exchange process. It is revealed that the formation of the bound state between H $1s$ and the valence orbitals, which enables resonant tunneling of the valence electron, and the rapid diffusion of the hole into the band are essential prerequisites for efficient neutralization leading to the complete absence of the surface peaks. Local charge equilibration is established for H^+ scattered from metal and semiconductor surfaces so that total neutralization occurs. On the other hand, for H^+ colliding with cations of the ionic compounds, although the resonance condition is satisfied with the valence band, equilibration does not occur easily due to insufficient mobility of the electron in the narrow band, resulting in inhibition of total neutralization. For H^+ scattering from negatively charged species such as O^{2-} and Cl^-, neutralization is suppressed to some extent due to the formation of the surface molecule. In terms of inelastic scattering, the occurrence of electron-hole-pair excitation and reionization can be elucidated from a combination of the RT process and the electron-promotion mechanism.

*Permanent address: Sherritt Technologies, Sherritt Inc., Fort Saskatchewan, Alberta, Canada T8L 3W4.

[1]H. D. Hagstrum, Phys. Rev. **94**, 336 (1954).

[2]W. Heiland and E. Taglauer, Nucl. Instrum. Methods **132**, 535 (1976).

[3]B. Brako and D. M. Newns, Rep. Prog. Phys. **52**, 655 (1989).

[4]J. Los and J. J. C. Geerlings, Phys. Rep. **190**, 133 (1990).

[5]R. Souda and M. Aono, Nucl. Instrum. Methods Phys. Res. Sect. B **15**, 114 (1986); R. Souda, T. Aizawa, C. Oshima, and Y. Ishizawa, *ibid.* **45**, 364 (1990).

[6]M. Shi, O. Grizzi, and J. W. Rabalais, Surf. Sci. **235**, 67 (1990).

[7]W. Eckstein, in *Inelastic Particle-Surface Collisions*, edited by E. Taglauer and W. Heiland, Springer Series in Chemical Physics Vol. 17 (Springer, New York, 1981), p.157.

[8]R. Souda, T. Aizawa, W. Hayami, S. Otani, and Y. Ishizawa, Phys. Rev. B **42**, 7761 (1990); **45**, 14 358 (1992); R. Souda, W. Hayami, T. Aizawa, and Y. Ishizawa, *ibid.* **50**, 1934 (1994).

[9]R. Souda, W. Hayami, T. Aizawa, S. Otani, and Y. Ishizawa, Phys. Rev. Lett. **69**, 192 (1992); R. Souda, W. Hayami, T. Aizawa, and Y. Ishizawa, Phys. Rev. B **48**, 17 255 (1993).

[10]R. Souda, Int. J. Mod. Phys. B **8**, 679 (1994).

[11]Y. Muda and T. Hanawa, Surf. Sci. **97**, 283 (1980).

[12]T. B. Grimly, V. C. Jyothi Bhasu, and K. L. Sebastian, Surf. Sci. **124**, 305 (1983).

[13]S. Tsuneyuki, N. Shima, and M. Tsukada, Surf. Sci. **186**, 26 (1987).

[14]Y. Muda and D. M. Newns, Phys. Rev. B **37**, 7048 (1988).

[15]H. Adachi, M. Tsukada, and C. Satoko, J. Phys. Soc. Jpn. **45**, 875 (1978).

[16]C. Satoko, M. Tsukada, and H. Adachi, J. Phys. Soc. Jpn. **45**, 1333 (1978).

[17]H. Nakanishi, H. Kasai, and A. Okiji, Surf. Sci. **197**, 515 (1988).

[18]V. Fano and W. Lichten, Phys. Rev. Lett. **14**, 627 (1965).

[19]M. Barat and W. Lichten, Phys. Rev. A **6**, 211 (1972).

[20]J. W. Rabalais, J. N. Chen, R. Kumar, and M. Nakayama, J. Chem. Phys. **83**, 6489 (1985).

[21]J. N. Chen and J. W. Rabalais, J. Am. Chem. Soc. **110**, 46 (1988).

[22]T. M. Buck, W. E. Wallace, P. A. Baragiola, G. H. Wheatley, J. B. Rothman, R. J. Gorte, and J. G. Tittensor, Phys. Rev. B **48**, 774 (1993).

[23]M. Tsukada, S. Tsuneyuki, and N. Shima, Surf. Sci. **164**, L811 (1985).

[24]S. Tsuneyuki and M. Tsukada, Phys. Rev. B **34**, 5758 (1986).

[25]R. Souda *et al.* (unpublished).

[26]B. Tilley *et al.* (unpublished).